

UDC 539.216.2: 537.52

DOI: 10.15587/1729-4061.2019.185674

Методом мікродугового оксидування технічно чистого алюмінію і алюмінію легового міддю і цинком в лужно-силикатном електроліті при щільності струму $\sim 20 \text{ A/дм}^2$ одержані покриття товщиною близько 100 мкм. Наведено результати дослідження морфології поверхні, фазового складу і твердості МДО-покриттів. Параметрами зміни служили склад електроліту і концентрація легуючих (Cu і Zn) елементів. Це дослідження проведено тому, що наявних в даний час даних не достатньо для уявлення про характер впливу хімічного складу алюмінієвого сплаву і умов електролізу (зокрема, складу електроліту) на механізм і кінетику перетворення $\gamma \rightarrow \alpha$. А без розуміння цього спрямована зміна структурного стану і властивостей МДО покриттів стає неможливою. В результаті досліджень було встановлено, що при мікродуговом оксидуванні алюмінієвих сплавів в лужному електроліті з додаванням рідкого скла (Na_2SiO_3) різної концентрації зміцнений шар складається з оксидів $\alpha\text{-Al}_2\text{O}_3$, $\gamma\text{-Al}_2\text{O}_3$ і муллита $3\text{Al}_2\text{O}_3 \cdot 2\text{SiO}_2$. Дані рентгеноструктурного аналізу покриттів свідчать про кристалічну будову покриттів. Встановлено, що легування алюмінію міддю і цинком істотно впливає на фазовий склад покриття, змінюючи кількісне співвідношення фаз нелінійним чином. Найбільший вміст $\alpha\text{-Al}_2\text{O}_3$ фази (до 60 об. %) досягається при легуванні Cu. При цьому найбільш висока твердість МДО покриттів досягається при використанні електроліту складу 1 г/л KOH і 6 г/л Na_2SiO_3 в алюмінієвих сплавах при вмісті міді більше 3 %, а цинку – 2–3 %. Встановлено, що механізм формування фазового складу слід пов'язати зі стабілізацією і дестабілізацією фази $\gamma\text{-Al}_2\text{O}_3$. З цього для досягнення високої твердості слід вибрати ті легуючі елементи, які впливають на дестабілізацію $\gamma\text{-Al}_2\text{O}_3$, що забезпечує утворення фази $\alpha\text{-Al}_2\text{O}_3$ (корунд). У зв'язку з цим виявлено, що катіони Cu^{2+} сприяють дестабілізації фази $\gamma\text{-Al}_2\text{O}_3$, а катіони Zn^{2+} призводять до стабілізації фази $\gamma\text{-Al}_2\text{O}_3$ при утриманні $\text{Zn} > 3 \%$.

Ключові слова: мікродугове оксидування, анодно-катодний режим, склад електроліту, легування, фазовий склад, корунд

DETERMINATION OF INFLUENCE OF ELECTROLYTE COMPOSITION AND IMPURITIES ON THE CONTENT OF $\alpha\text{-Al}_2\text{O}_3$ PHASE IN MAO-COATINGS ON ALUMINUM

V. Subbotina

PhD, Associate Professor*

E-mail: subbotina.valeri@gmail.com

Ubeidulla F. Al-Qawabeha

PhD, Associate Professor**

E-mail: ubeid1@yahoo.com

V. Belozarov

PhD, Professor*

O. Sobol'

Doctor of Physical and

Mathematical Sciences, Professor*

E-mail: sool@kpi.kharkov.ua

A. Subbotin

Researcher*

E-mail: subbotina.valeri@gmail.com

Taha A. Tabaza

PhD, Associate Professor**

Safwan M. Al-Qawabah

PhD, Associate Professor, Dean-Faculty of Engineering and Technology**

E-mail: safwan1q@gmail.com

*Department of Materials Science

National Technical University «Kharkiv Polytechnic Institute»

Kyrpychova str., 2, Kharkiv, Ukraine, 61002

**Department of Mechanical Engineering

Al-Zaytoonah University

Queen Alia Airport str., 594, Amman, Jordan, 11733

Received date 07.10.2019

Accepted date 20.11.2019

Published date 26.12.2019

Copyright © 2019, V. Subbotina, Ubeidulla F. Al-Qawabeha, V. Belozarov, O. Sobol',

A. Subbotin, Taha A. Tabaza, Safwan M. Al-Qawabah

This is an open access article under the CC BY license (<http://creativecommons.org/licenses/by/4.0>)

1. Introduction

The surface condition of functional materials largely determines their properties [1, 2]. Therefore, at present, struc-

tural surface engineering is the main method for achieving high functional properties of materials [3, 4]. The basis of modern methods of structural engineering of a surface is its modification under highly nonequilibrium conditions [5, 6].

In most technologies, such a modification leads to a decrease in the grain size of crystallites to a nanometer size [7, 8]. To increase the stability of such metastable states, two approaches are used: doping to low concentrations (up to 1 at %) [9, 10] and multi-element doping in a ratio of elements close to equiatomic [11, 12]. Moreover, the highest mechanical properties were achieved by obtaining plasma flows on the surface of coatings [13, 14].

One of the most promising methods in this direction is plasma oxidation [15, 16]. The use of this method shows the greatest efficiency for obtaining highly hard protective coatings on valve materials (Al, Ti, Mg, Ta, Nb, Zr) [17, 18]. Such a process is called microarc oxidation (MAO) [19, 20]. Microarc oxidation refers to the high-voltage anodizing method [21, 22]. The differences between the MAO method and the anodization process include the use of not direct current, but alternating [23, 24] with surge [25] currents. The differences also include the use of weakly alkaline electrolytes (using the MAO method) instead of acid ones, which are mainly used for anodizing [26, 27]. However, the main distinguishing feature is the use of the energy of electrical microdischarges that randomly migrate over the surface of products processed in the electrolyte. These microdischarges have a thermal and plasmochemical effect on the coating itself and electrolyte [28, 29]. As a result, the hardness and strength of materials increase [30, 31].

In recent years, there has been an increased interest to light metal elements (to a large extent this relates to Al and Ti) as structural elements of aerospace equipment and engines of various modifications. In this regard, the technologies that lead to an increase in the strength and hardness of these materials are relevant and demanded by the industry.

2. Literature review and problem statement

The work [32] describes the microarc oxidation process for creating an oxide film on the surface of metals and alloys by their anodic polarization in a conducting medium. It was shown that microarc oxidation is accompanied by the formation of microplasma [33] and microregions with high pressure due to the gases formed [34, 35]. This leads to the occurrence of high-temperature chemical transformations [36, 37] and the transport of substance in the arc [38, 39].

In addition, a comparison of the MAO method with anodization shows that when anodizing, the size of the part increases by a film thickness of 30–60 μm . At the same time, in order to obtain it, it is necessary to observe the temperature regime. For this, the current density should not exceed 2.5 A/dm². Microarc oxidation allows increasing current density up to 100 A/dm². Due to this factor, the duration of the process is reduced by 20 times.

Microarc oxidation allows obtaining multifunctional coatings with a unique set of properties (high wear resistance, corrosion resistance, heat resistance) [40, 41].

MAO coatings obtained on aluminum and its alloys in silicate-alkaline electrolytes, as a rule, have a three-layer structure (transition layer, main working layer, technological layer) and uneven distribution of components [42].

It is possible to change the phase composition and control polymorphic transformations based on aluminum oxide not only due to changes in electrolysis conditions, but also by optimizing the composition used to obtain coatings [43, 44]. The presence of direct contact between the metal and the

breakdown region allows expecting a large effect of the chemical composition of the aluminum alloy on the properties of coatings [45]. Preliminary studies have shown that the phase composition of coatings on different grades of aluminum alloys is different, which is apparently due to the partial completion of the transformation of the low-temperature modification of $\gamma\text{-Al}_2\text{O}_3$ alumina into the stable modification $\alpha\text{-Al}_2\text{O}_3$ [31, 35].

Therefore, to achieve high hardness and wear resistance of MAO coatings on aluminum alloys, it is necessary to provide a large percentage of the $\alpha\text{-Al}_2\text{O}_3$ (corundum) phase. Moreover, as was established in [31, 35], phase formation during the MAO treatment of aluminum alloys in the microarc discharge mode begins with the $\gamma\text{-Al}_2\text{O}_3$ phase, which undergoes the $\gamma \rightarrow \alpha$ transition as the coating forms.

However, as follows from the literature review, the main attention is mainly paid to the influence of technological parameters on the properties of the modified surface. Detailed studies of structural states and the influence of processing conditions on them are practically absent. This is due to the fact that industrial alloys with multi-element alloying are mainly studied, which makes it practically impossible to establish the laws of the influence of elemental composition on the mechanism and kinetics of structural transformations. Since the influence of different elements (making up the alloy) can have not only different kinetics, but also lead to opposite effects (as assumed, for example, from the results of [31]). Because of this, there are currently insufficient data to understand the nature of the influence of the chemical composition of the aluminum alloy and electrolysis conditions (in particular, electrolyte composition) on the mechanism and kinetics of both the main $\gamma \rightarrow \alpha$ transformation and other types of transformations. And without understanding this, a directed change in the structural state and properties of MAO coatings becomes impossible.

3. The aim and objectives of the study

The aim of the work is to study the laws of the influence of the electrolyte composition and doping of aluminum with Cu and Zn atoms on the phase formation processes, structure and hardness of coatings formed in an alkaline silicate electrolyte in the anodic-cathodic mode of the microarc oxidation process.

To achieve this goal, the following tasks were solved:

- to determine the phase composition of coatings during microarc oxidation of aluminum alloys doped with Zn and Cu;
- to establish the dependence of the coating hardness on the content of alloying elements and electrolyte composition;
- to analyze and explain the revealed patterns in terms of stabilization and destabilization of phases in alloys and determine the effect of Cu and Zn impurity atoms on this process.

4. Conditions for obtaining microarc oxide coatings on aluminum alloys and methods for their research

4.1. Conditions for obtaining microarc oxide coatings on aluminum alloys

To obtain microarc oxide coatings, samples of aluminum alloys in the form of cylinders with a diameter of 20 mm and a height of 10 mm were used. The treatment was carried out

in an alkaline electrolyte with the addition of liquid glass (Na_2SiO_3). The MAO treatment was carried out in the anode-cathode mode at a current density of $\sim 20 \text{ A/dm}^2$, the treatment time was $\tau=1$ hour (to study the morphology of the initial stage of coating growth, $\tau=10$ min was used). A capacitor-type power supply was used. In order to optimize the technology, the MAO treatment was carried out in electrolytes of two different compositions – $1 \text{ g/l KOH} + 6 \text{ g/l Na}_2\text{SiO}_3$ and $2 \text{ g/l KOH} + 12 \text{ g/l Na}_2\text{SiO}_3$. These electrolytes are the most versatile for organizing the anode-cathode process in the microarc discharge mode.

Technically pure aluminum, copper-doped (from 3 to 9 % Cu) aluminum and zinc-doped (from 1 to 10 % Zn) aluminum were subjected to microarc treatment. It should be noted that copper and zinc are the main components of deformable aluminum alloys, hardened by heat treatment.

4. 2. X-ray quantitative phase analysis

X-ray diffraction survey of the samples was carried out on a DRON-3 diffractometer (Burevesnik, Russia) in monochromatized radiation from a copper anode in the range of angles $2\theta=10-70^\circ$. Scanning was carried out point by point with a step of 0.1 degree and accumulation time of 10 seconds at a point. Quantitative phase analysis was carried out using reference samples. The relative error in determining the phase content by this method depends on the integrated intensity of the diffraction peaks. Therefore, to reduce the error in determining the composition, not all diffraction peaks of the phases were used, but only the most intense (in their reflectivity). This technique improves accuracy, but does not allow the use of statistical processing over the entire spectrum.

4. 3. Microhardness measurement method

The microhardness of the samples was determined on a PMT-3 instrument (AO LOMO, Russia). Microhardness was determined by the indentation of an indenter – a diamond pyramid, with a square base and a tetrahedral shape with an angle at the apex between the opposite sides of the pyramid equal to 136° . The microhardness number of the tetrahedral pyramid with a square base H , kg/mm^2 , was determined by the formula (1):

$$H = \frac{P}{S} = \frac{1P \cdot \sin \frac{\alpha}{2}}{d^2} = 1.8544 \frac{P}{d^2}, \quad (1)$$

where P is the nominal load applied to the diamond pyramid; S is the conditional area of the side surface of the imprint, mm^2 ; d is the arithmetic mean of the length of both diagonals of the square imprint, mm ; α is the point angle of the diamond pyramid, deg .

When analyzing the obtained results, the average value over 5 measurements was used.

4. 4. Thickness control of coatings obtained by micro-arc oxidation

To measure the thickness of oxide films, the non-destructive testing method, the electromagnetic method, was used. In this case, the coating thickness was measured on a VT-10NTs instrument (Kontrolpribor, Russia). Metallographic analysis of transverse sections on an Axio Vert.A1 MAT device (Carl Zeiss, Germany) was also used for thickness control.

5. Results of the study of the influence of MAO treatment regimes on the surface morphology and phase composition of coatings of aluminum alloys doped with Zn and Cu

The control of the coating thickness showed that in one hour of processing, a coating is formed with a thickness of $100-110$ microns. The metallography of the surface revealed that in the process of coating formation, the surface morphology changes significantly. At the beginning of the process, a light gray coating with a small roughness is formed (Fig. 1, *a*). With an increase in the process duration, the surface morphology changes – the roughness and size of microroughness increase, and the places of melting are clearly visible (Fig. 1, *b*). The change in the surface morphology during the oxidation process is due to the change in the density and power of microdischarges. As can be seen during visual observation of the MAO process, the initial stages are characterized by a high density of low-power discharges (relatively low luminosity). As the coating thickness increases, the density of the discharges decreases, and their power increases. The latter was determined by an increase in luminosity.

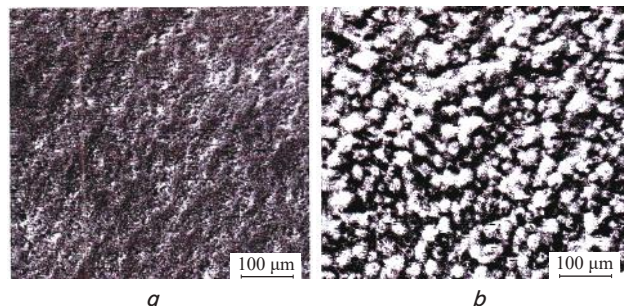


Fig. 1. Surface morphology of the oxide coating on the aluminum alloy Al+9 % Cu:
a – $\tau=10$ min; *b* – $\tau=1$ hour

It is known that the properties of MAO coatings (base layer) are primarily determined by their phase composition [31, 35].

The X-ray phase analysis carried out in the work revealed the effect of doping on the phase composition of the coatings. Typical diffraction patterns of the coatings are shown in Fig. 2.

It can be seen that as a result of microarc oxidation of aluminum alloys in an alkaline electrolyte with the addition of liquid glass (Na_2SiO_3) of various concentrations, the hardened layer consists of the oxides $\alpha\text{-Al}_2\text{O}_3$, $\gamma\text{-Al}_2\text{O}_3$ and mullite $3\text{Al}_2\text{O}_3 \cdot 2\text{SiO}_2$. The quantitative ratio between these phases depends on the oxidation mode, electrolyte composition and chemical composition of the oxidized alloy.

The spectra presented in Fig. 2 show that the hardened layer on all the studied samples has a crystalline structure. The relative intensity of the diffraction lines for the identified phases is close to the table data, which indicates the absence of a pronounced texture (i. e., the random orientation of the crystals of the hardened layer). The hardened layer has a similar phase composition, but the quantitative ratio is determined by the extent of aluminum alloying (Fig. 3).

As can be seen from Fig. 3, the highest content of the $\alpha\text{-Al}_2\text{O}_3$ phase is observed in Al+Cu alloys with a Cu content of about 4 wt. % (Fig. 3, *a, b*). For such a content, microarc treatment in an electrolyte of 2 g/l KOH and $12 \text{ g/l Na}_2\text{SiO}_3$ leads to a content of about 30 vol %

α - Al_2O_3 (Fig. 3, *b*). When 1 g/l KOH and 6 g/l Na_2SiO_3 are treated in an electrolyte, the α - Al_2O_3 phase content in the coating reaches 60 vol %.

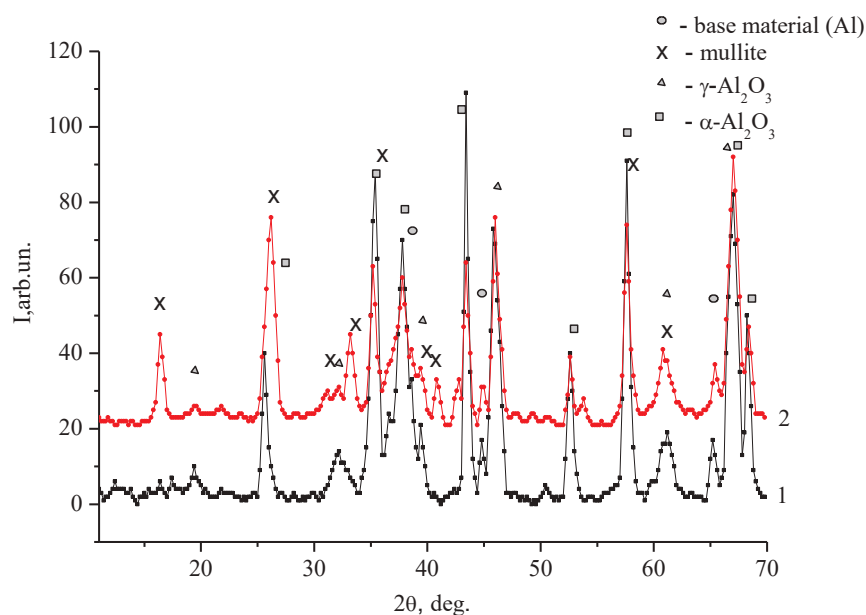


Fig. 2. X-ray diffraction patterns of Al+9 % Cu samples after MAO treatment in an electrolyte: 1 – 1 g/l KOH and 6 g/l Na_2SiO_3 , 2 – 2 g/l KOH and 12 g/l Na_2SiO_3

6. Results of the study of the effect of electrolyte composition and alloying on the hardness of aluminum alloys after MAO treatment

The highest physical and mechanical properties and the highest hardness (about 24 GPa) are in the α - Al_2O_3 phase (corundum). The γ - Al_2O_3 phase has a hardness of about 14 GPa, and mullite has a hardness close to 10 GPa. In this regard, the production of coatings with high hardness is associated with the need to ensure a high percentage of α - Al_2O_3 in the coating composition.

The obtained dependences of hardness on the alloy composition are shown in Fig. 4.

Fig. 4 shows that the dependence of hardness on composition is non-monotonic. A significant increase in hardness in the case of an Al+Cu alloy is manifested when the Cu content is $>3\%$. In the case of an Al+Zn alloy, the maximum hardness is at a Zn content of $\sim 3\%$. These results were obtained in an electrolyte with a composition of 1 g/l KOH + 6 g/l Na_2SiO_3 .

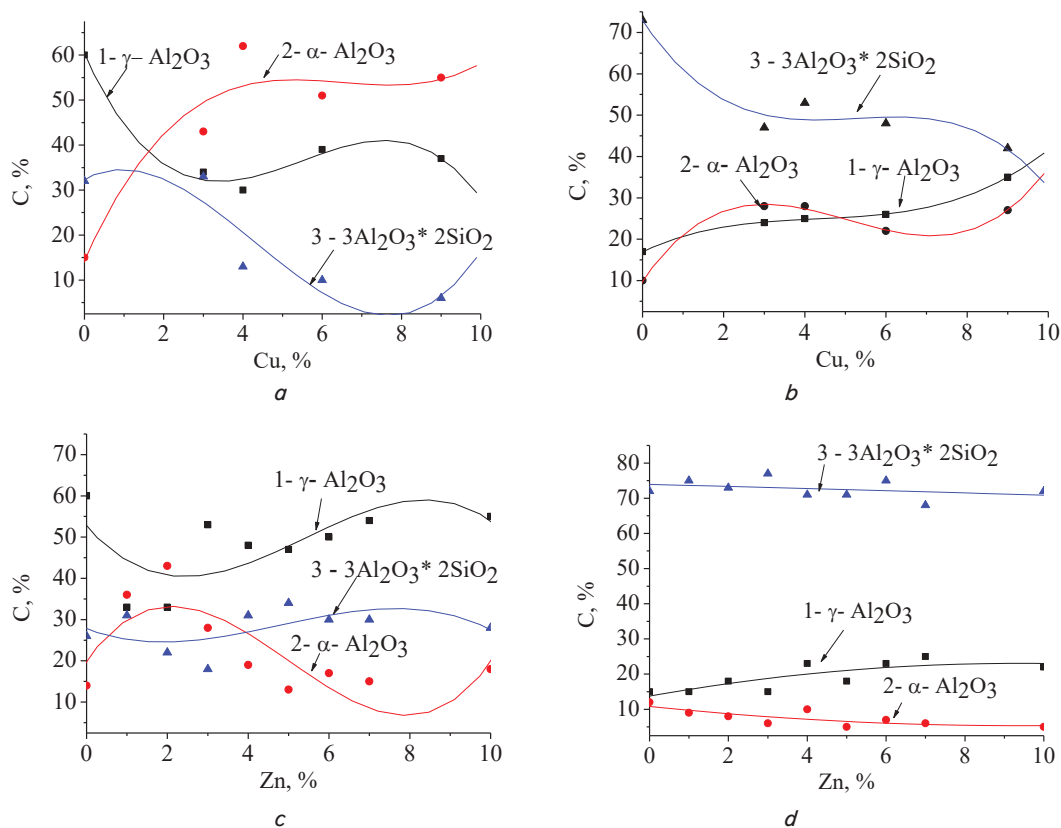


Fig. 3. Dependences of the phase composition of the coating on the concentration of the alloying element in Al+Cu and Al+Zn alloys: *a* – Al+Cu, electrolyte 1 g/l KOH and 6 g/l Na_2SiO_3 ; *b* – Al+Cu, electrolyte 2 g/l KOH and 12 g/l Na_2SiO_3 ; *c* – Al+Zn, electrolyte 1 g/l KOH and 6 g/l Na_2SiO_3 ; *d* – Al+Zn, electrolyte 2 g/l KOH and 12 g/l Na_2SiO_3 ; 1 – γ - Al_2O_3 ; 2 – α - Al_2O_3 ; 3 – $3\text{Al}_2\text{O}_3 \cdot 2\text{SiO}_2$ (mullite)

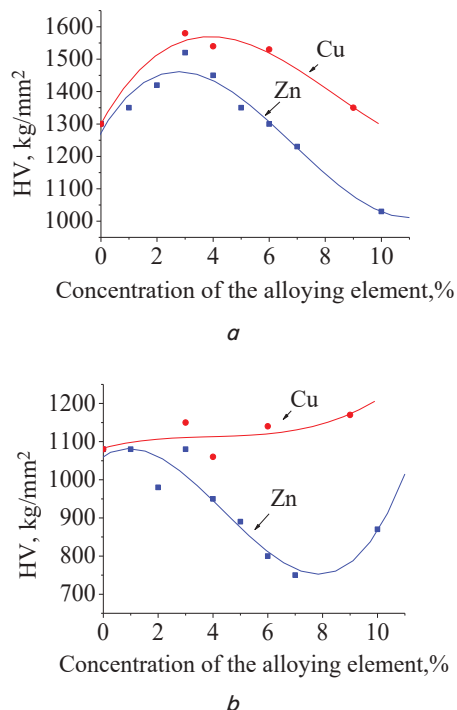


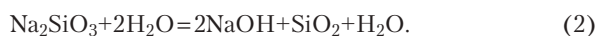
Fig. 4. Dependences of hardness on the concentration of alloying elements Cu and Zn:
a – electrolyte 1 g/l KOH and 6 g/l Na₂SiO₃;
b – electrolyte 2 g/l KOH and 12 g/l Na₂SiO₃

The use of an electrolyte with an increase in the water glass content (12 g/l Na₂SiO₃) significantly reduces the coating hardness due to the presence of mullite in the coating (the content of which exceeds 50 %).

7. Discussion of the research results on the effect of electrolyte composition and alloying on the phase-structural state and hardness of MAO coatings

The research results showed that although the addition of Na₂SiO₃ to the electrolyte provides a significant increase in the thickness of the formed coatings, it is accompanied by the appearance of a phase with low hardness (mullite) – 3Al₂O₃·2SiO₂ (Fig. 2, 3).

The formation of mullite is determined by the fact that when liquid glass is diluted with water, hydrolysis occurs by the reaction:



The interaction of γ -Al₂O₃ with SiO₂ leads to the appearance of mullite:



The data obtained in the work indicate that the main phase of the coating is the γ -Al₂O₃ phase. The phase composition of the coatings of the studied alloys differs both quantitatively and qualitatively (Fig. 2, 3). The analysis of the results shows that the mechanism of formation of the phase composition should be associated with stabilization and destabilization of the γ -Al₂O₃ phase.

As shown by precision studies (from the data on the position of the peaks in Fig. 2), the lattice period of the γ -Al₂O₃ phase varies depending on the degree of aluminum doping (Fig. 5). For the coating on aluminum, the lattice period is 0.790 nm, which corresponds to the table value. With an increase in alloying degree, an increase in the lattice period is observed, both in the case of copper alloying and in the case of zinc alloying.

The results obtained indicate that the γ -Al₂O₃ phase is doped with impurity atoms by the substitution type. The change in the lattice period in this case will be determined, on the one hand, by the difference between the ionic radii of Al³⁺ ($r=0.067$ nm) and the ionic radii of Cu²⁺ ($r=0.087$ nm) and Zn²⁺ ($r=0.086$ nm), and, on the other hand, by the difference in valency and concentration of the dissolved component. Comparing the ionic radius of Al with the ionic radius of impurity cations, we can conclude that the Cu and Zn cations should lead to an increase in the lattice period of the γ -Al₂O₃ phase.

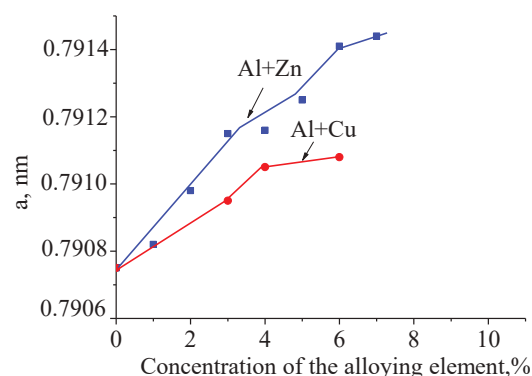


Fig. 5. Effect of alloying aluminum with copper (Al+Cu) and zinc (Al+Zn) on the lattice period of the γ -Al₂O₃ phase

The analysis of the results presented in Fig. 3, 5 indicate that Cu²⁺ cations contribute to the destabilization of the γ -Al₂O₃ phase, and Zn²⁺ cations lead to stabilization of the γ -Al₂O₃ phase at a Zn content >3. Destabilization (or stabilization) is determined by the effect on the γ -Al₂O₃→ α -Al₂O₃ transition based on the phase composition data (Fig. 3). A comparison with the results of hardness measurements (Fig. 4) shows that the achievement of a high hardness of MAO coatings on aluminum alloys is associated with the need to ensure a high α -Al₂O₃ phase content. In the case of zinc doping of aluminum, an extreme dependence of the α -Al₂O₃ phase content on zinc concentration is observed. The maximum α -Al₂O₃ phase content corresponds to 2 % Zn. At present, it is difficult to explain the resulting extreme dependence. Although it can be assumed that a significant effect of impurities on the formation of α -Al₂O₃ from γ -Al₂O₃ can be determined by their adsorption on the surface of alumina particles. This leads to regulation of the nucleation rate during the growth of new phase grains. However, to substantiate this assumption, additional studies are required, which are planned to be carried out in the future.

7. Conclusions

1. The data of x-ray diffraction analysis of the coatings indicate the crystal structure of the coatings. The phase composition consists of aluminum oxides α -Al₂O₃ (corundum),

γ - Al_2O_3 and mullite $3\text{Al}_2\text{O}_3 \cdot 2\text{SiO}_2$, which provide high hardness of coatings ($\text{HV} > 1,000 \text{ kg/mm}^2$). It was established that copper and zinc alloying of aluminum significantly affects the phase composition of the coating, changing the quantitative ratio of the phases in a nonlinear manner. The highest content of the α - Al_2O_3 phase (up to 60 vol. %) is achieved by Cu doping.

2. It is shown that high hardness of coatings on aluminum alloys is ensured when the copper content is more than 3 %, and zinc – 2–3 %. The highest hardness of the MAO coatings is achieved using an electrolyte of 1 g/l KOH and 6 g/l Na_2SiO_3 .

3. It is established that the mechanism of formation of the phase composition should be associated with stabilization and destabilization of the γ - Al_2O_3 phase. Therefore, to achieve high hardness, it is necessary to choose those alloying elements that affect the destabilization of γ - Al_2O_3 , which

ensures the formation of the α - Al_2O_3 phase (corundum). In this regard, it was found that Cu^{2+} cations contribute to the destabilization of the γ - Al_2O_3 phase, and Zn^{2+} cations lead to stabilization of the γ - Al_2O_3 phase at a Zn content $> 3 \%$.

Acknowledgments

The authors would like to express gratitude to the Al-Zaytoonah University of Jordan for financial support under the project (19/18/2018–2019), as well as the Ministry of Education and Science of Ukraine for financial support under the project «Development of materials science for the use of high-performance ion-plasma technologies for three-level surface engineering» (state registration number No. 0118U002044).

References

1. Radionenko, O., Kindrachuk, M., Tisov, O., Kryzhanovskiy, A. (2018). Features of transition modes of friction surfaces with partially regular microrelief. *Aviation*, 22 (3), 86–92. doi: <https://doi.org/10.3846/aviation.2018.6204>
2. Panarin, V. Y., Svavil'nyy, M. Y., Khomynych, A. I., Kindrachuk, M. V., Kornienko, A. O. (2017). Creation of a Diffusion Barrier at the Interphase Surface of Composite Coatings Reinforced with Carbon Nanotubes. *Journal of Nano- and Electronic Physics*, 9 (6), 06023-1–06023-5. doi: [https://doi.org/10.21272/jnep.9\(6\).06023](https://doi.org/10.21272/jnep.9(6).06023)
3. Sobol', O. V., Andreev, A. A., Gorban', V. F., Meylekhov, A. A., Postelnyk, H. O. (2016). Structural Engineering of the Vacuum Arc ZrN/CrN Multilayer Coatings. *Journal of Nano- and Electronic Physics*, 8 (1), 01042-1–01042-5. doi: [https://doi.org/10.21272/jnep.8\(1\).01042](https://doi.org/10.21272/jnep.8(1).01042)
4. Sobol', O. V. (2016). Structural Engineering Vacuum-plasma Coatings Interstitial Phases. *Journal of Nano- and Electronic Physics*, 8 (2), 02024-1–02024-7. doi: [https://doi.org/10.21272/jnep.8\(2\).02024](https://doi.org/10.21272/jnep.8(2).02024)
5. Mayrhofer, P. H., Mitterer, C., Hultman, L., Clemens, H. (2006). Microstructural design of hard coatings. *Progress in Materials Science*, 51 (8), 1032–1114. doi: <https://doi.org/10.1016/j.pmatsci.2006.02.002>
6. Sobol', O. V., Andreev, A. A., Gorban', V. F. (2016). Structural Engineering of Vacuum-ARC Multiperiod Coatings. *Metal Science and Heat Treatment*, 58 (1-2), 37–39. doi: <https://doi.org/10.1007/s11041-016-9961-3>
7. Morton, B. D., Wang, H., Fleming, R. A., Zou, M. (2011). Nanoscale Surface Engineering with Deformation-Resistant Core–Shell Nanostructures. *Tribology Letters*, 42 (1), 51–58. doi: <https://doi.org/10.1007/s11249-011-9747-0>
8. Barmin, A. E., Zubkov, A. I., Il'inskii, A. I. (2012). Structural features of the vacuum condensates of iron alloyed with tungsten. *Functional Materials*, 19 (2), 256–259.
9. Glushchenko, M. A., Belozyorov, V. V., Sobol', O. V., Subbotina, V. V., Zelenskaya, G. I. (2017). Effect of Tantalum on the Texture of Copper Vacuum Condensates. *Journal of Nano- and Electronic Physics*, 9 (2), 02015-1–02015-5. doi: [https://doi.org/10.21272/jnep.9\(2\).02015](https://doi.org/10.21272/jnep.9(2).02015)
10. Glushchenko, M. A., Lutsenko, E. V., Sobol', O. V., Barmin, A. E., Zubkov, A. I. (2016). The Influence of Copper Condensates Alloying with Co, Mo, Ta Transition Metals on the Structure and the Hall-Petch Dependence. *Journal of Nano- and Electronic Physics*, 8(3), 03015-1–03015-4. doi: [https://doi.org/10.21272/jnep.8\(3\).03015](https://doi.org/10.21272/jnep.8(3).03015)
11. Krause-Rehberg, R., Pogrebnyak, A. D., Borisyuk, V. N., Kaverin, M. V., Ponomarev, A. G., Bilokur, M. A. et. al. (2013). Analysis of local regions near interfaces in nanostructured multicomponent (Ti-Zr-Hf-V-Nb)N coatings produced by the cathodic-arc-vapor-deposition from an arc of an evaporating cathode. *The Physics of Metals and Metallography*, 114 (8), 672–680. doi: <https://doi.org/10.1134/s0031918x13080061>
12. Sobol', O. V., Andreev, A. A., Gorban', V. F., Krapivka, N. A., Stolbovoi, V. A., Serdyuk, I. V., Fil'chikov, V. E. (2012). Reproducibility of the single-phase structural state of the multielement high-entropy Ti-V-Zr-Nb-Hf system and related superhard nitrides formed by the vacuum-arc method. *Technical Physics Letters*, 38 (7), 616–619. doi: <https://doi.org/10.1134/s1063785012070127>
13. Sobol', O. V., Meylekhov, A. A. (2018). Conditions of Attaining a Superhard State at a Critical Thickness of Nanolayers in Multi-periodic Vacuum-Arc Plasma Deposited Nitride Coatings. *Technical Physics Letters*, 44 (1), 63–66. doi: <https://doi.org/10.1134/s1063785018010224>
14. Sobol', O. V., Postelnyk, A. A., Meylekhov, A. A., Andreev, A. A., Stolbovoy, V. A. (2017). Structural Engineering of the Multilayer Vacuum Arc Nitride Coatings Based on Ti, Cr, Mo and Zr. *Journal of Nano- and Electronic Physics*, 9 (3), 03003-1–03003-6. doi: [https://doi.org/10.21272/jnep.9\(3\).03003](https://doi.org/10.21272/jnep.9(3).03003)
15. Nashrah, N., Kamil, M. P., Yoon, D. K., Kim, Y. G., Ko, Y. G. (2019). Formation mechanism of oxide layer on AZ31 Mg alloy subjected to micro-arc oxidation considering surface roughness. *Applied Surface Science*, 497, 143772. doi: <https://doi.org/10.1016/j.apsusc.2019.143772>

16. Muhaffel, F., Kaba, M., Cempura, G., Derin, B., Kruk, A., Atar, E., Cimenoglu, H. (2019). Influence of alumina and zirconia incorporations on the structure and wear resistance of titania-based MAO coatings. *Surface and Coatings Technology*, 377, 124900. doi: <https://doi.org/10.1016/j.surfcoat.2019.124900>
17. Yerokhin, A. L., Nie, X., Leyland, A., Matthews, A., Dowey, S. J. (1999). Plasma electrolysis for surface engineering. *Surface and Coatings Technology*, 122 (2-3), 73–93. doi: [https://doi.org/10.1016/s0257-8972\(99\)00441-7](https://doi.org/10.1016/s0257-8972(99)00441-7)
18. Wang, S., Xie, F., Wu, X. (2017). Mechanism of Al₂O₃ coating by cathodic plasma electrolytic deposition on TiAl alloy in Al(NO₃)₃ ethanol-water electrolytes. *Materials Chemistry and Physics*, 202, 114–119. doi: <https://doi.org/10.1016/j.matchemphys.2017.09.006>
19. Yang, Y., Gu, Y., Zhang, L., Jiao, X., Che, J. (2017). Influence of MAO Treatment on the Galvanic Corrosion Between Aluminum Alloy and 316L Steel. *Journal of Materials Engineering and Performance*, 26 (12), 6099–6106. doi: <https://doi.org/10.1007/s11665-017-3037-4>
20. Zhang, X., Li, C., Yu, Y., Lu, X., Lv, Y., Jiang, D. et. al. (2019). Characterization and property of bifunctional Zn-incorporated TiO₂ micro-arc oxidation coatings: The influence of different Zn sources. *Ceramics International*, 45 (16), 19747–19756. doi: <https://doi.org/10.1016/j.ceramint.2019.06.228>
21. Zong, Y., Cao, G. P., Hua, T. S., Cai, S. W., Song, R. G. (2019). Effects of electrolyte system on the microstructure and properties of MAO ceramics coatings on 7050 high strength aluminum alloy. *Anti-Corrosion Methods and Materials*, 66 (6), 812–818. doi: <https://doi.org/10.1108/acmm-02-2019-2083>
22. Sedelnikova, M. B., Komarova, E. G., Sharkeev, Y. P., Ugodchikova, A. V., Mushtovatova, L. S., Karpova, M. R. et. al. (2019). Zn²⁺, Cu²⁺ or Ag-incorporated micro-arc coatings on titanium alloys: Properties and behavior in synthetic biological media. *Surface and Coatings Technology*, 369, 52–68. doi: <https://doi.org/10.1016/j.surfcoat.2019.04.021>
23. Dehghanghadikolaei, A., Ibrahim, H., Amerinatanzi, A., Hashemi, M., Moghaddam, N. S., Elahinia, M. (2019). Improving corrosion resistance of additively manufactured nickel – titanium biomedical devices by micro-arc oxidation process. *Journal of Materials Science*, 54 (9), 7333–7355. doi: <https://doi.org/10.1007/s10853-019-03375-1>
24. Zlotnikov, I. I., Shapovalov, V. M. (2019). Improving the Antifriction Properties of Ceramic Coatings Obtained by the Method of MAO on Aluminum Alloys. *Journal of Friction and Wear*, 40 (5), 360–363. doi: <https://doi.org/10.3103/s1068366619050222>
25. Shao, Q., Jiang, B., Huang, S. (2019). A comparative study on the microstructure and corrosion resistance of MAO coatings prepared in alkaline and acidic electrolytes. *Materials Research Express*, 6 (8), 0865b4. doi: <https://doi.org/10.1088/2053-1591/ab2014>
26. Li, G., Wang, Y., Qiao, L., Zhao, R., Zhang, S., Zhang, R. et. al. (2019). Preparation and formation mechanism of copper incorporated micro-arc oxidation coatings developed on Ti-6Al-4V alloys. *Surface and Coatings Technology*, 375, 74–85. doi: <https://doi.org/10.1016/j.surfcoat.2019.06.096>
27. Huang, H., Qiu, J., Sun, M., Liu, W., Wei, X. (2019). Morphological evolution and burning behavior of oxide coating fabricated on aluminum immersed in etidronic acid at high current density. *Surface and Coatings Technology*, 374, 83–94. doi: <https://doi.org/10.1016/j.surfcoat.2019.05.081>
28. Gecu, R., Yurekturk, Y., Tekoglu, E., Muhaffel, F., Karaaslan, A. (2019). Improving wear resistance of 304 stainless steel reinforced AA7075 aluminum matrix composite by micro-arc oxidation. *Surface and Coatings Technology*, 368, 15–24. doi: <https://doi.org/10.1016/j.surfcoat.2019.04.029>
29. Yang, X., Chen, L., Jin, X., Du, J., Xue, W. (2019). Influence of temperature on tribological properties of microarc oxidation coating on 7075 aluminium alloy at 25 °C–300 °C. *Ceramics International*, 45 (9), 12312–12318. doi: <https://doi.org/10.1016/j.ceramint.2019.03.146>
30. Belozеров, V., Mahatlova, A., Sobol', O., Subbotina, V., Subbotin, A. (2017). Improvement of energy efficiency in the operation of a thermal reactor with submerged combustion apparatus through the cyclic input of energy. *Eastern-European Journal of Enterprise Technologies*, 2 (5 (86)), 39–43. doi: <https://doi.org/10.15587/1729-4061.2017.96721>
31. Belozеров, V., Sobol, O., Mahatlova, A., Subbotina, V., Tabaza, T. A., Al-Qawabeha, U. F., Al-Qawabah, S. M. (2017). The influence of the conditions of microplasma processing (microarc oxidation in anodecathode regime) of aluminum alloys on their phase composition. *Eastern-European Journal of Enterprise Technologies*, 5 (12 (89)), 52–57. doi: <https://doi.org/10.15587/1729-4061.2017.112065>
32. Tihonenko, V. V., Shkil'ko, A. M. (2012). Method of microarc oxidation. *Eastern-European Journal of Enterprise Technologies*, 2 (13 (56)), 13–18. Available at: <http://journals.uran.ua/eejet/article/view/3940/3608>
33. Curran, J. A., Clyne, T. W. (2005). Thermo-physical properties of plasma electrolytic oxide coatings on aluminium. *Surface and Coatings Technology*, 199 (2-3), 168–176. doi: <https://doi.org/10.1016/j.surfcoat.2004.09.037>
34. Martin, J., Nominé, A. V., Stef, J., Nominé, A., Zou, J. X., Henrion, G., Grosdidier, T. (2019). The influence of metallurgical state of substrate on the efficiency of plasma electrolytic oxidation (PEO) process on magnesium alloy. *Materials & Design*, 178, 107859. doi: <https://doi.org/10.1016/j.matdes.2019.107859>
35. Belozеров, V., Sobol, O., Mahatlova, A., Subbotina, V., Tabaza, T. A., Al-Qawabeha, U. F., Al-Qawabah, S. M. (2018). Effect of electrolysis regimes on the structure and properties of coatings on aluminum alloys formed by anodecathode micro arc oxidation. *Eastern-European Journal of Enterprise Technologies*, 1 (12 (91)), 43–47. doi: <https://doi.org/10.15587/1729-4061.2018.121744>

36. Subbotina, V. V., Sobol, O. V., Belozero, V. V., Makhatilova, A. I., Shnayder, V. V. (2019). Use of the Method of Micro-arc Plasma Oxidation to Increase the Antifriction Properties of the Titanium Alloy Surface. *Journal of Nano- and Electronic Physics*, 11 (3), 03025-1–03025-5. doi: [https://doi.org/10.21272/jnep.11\(3\).03025](https://doi.org/10.21272/jnep.11(3).03025)
37. Madhavi, Y., Rama Krishna, L., Narasaiah, N. (2019). Influence of micro arc oxidation coating thickness and prior shot peening on the fatigue behavior of 6061-T6 Al alloy. *International Journal of Fatigue*, 126, 297–305. doi: <https://doi.org/10.1016/j.ijfatigue.2019.05.013>
38. Li, C.-Y., Feng, X.-L., Fan, X.-L., Yu, X.-T., Yin, Z.-Z., Kannan, M. B. et. al. (2019). Corrosion and Wear Resistance of Micro-Arc Oxidation Composite Coatings on Magnesium Alloy AZ31–The Influence of Inclusions of Carbon Spheres. *Advanced Engineering Materials*, 21 (9), 1900446. doi: <https://doi.org/10.1002/adem.201900446>
39. Lai, P., Zhang, H., Zhang, L., Zeng, Q., Lu, J., Guo, X. (2019). Effect of micro-arc oxidation on fretting wear behavior of zirconium alloy exposed to high temperature water. *Wear*, 424-425, 53–61. doi: <https://doi.org/10.1016/j.wear.2019.02.001>
40. Zhang, Y., Chen, F., Zhang, Y., Liu, Z., Wang, X., Du, C. (2019). Influence of graphene oxide on the antiwear and antifriction performance of MAO coating fabricated on Mg Li alloy. *Surface and Coatings Technology*, 364, 144–156. doi: <https://doi.org/10.1016/j.surfcoat.2019.01.103>
41. Lesnevskiy, L. N., Lyakhovetskiy, M. A., Kozhevnikov, G. D., Ushakov, A. M. (2019). Research of the AK4-1 alloy microarc oxidation modes effect on the composite ceramic coatings erosion resistance. *Journal of Physics: Conference Series*, 1281, 012048. doi: <https://doi.org/10.1088/1742-6596/1281/1/012048>
42. Hua, T. S., Song, R. G., Zong, Y., Cai, S. W., Wang, C. (2019). Effect of solution pH on stress corrosion and electrochemical behaviour of aluminum alloy with micro-arc oxidation coating. *Materials Research Express*, 6 (9), 096441. doi: <https://doi.org/10.1088/2053-1591/ab30fc>
43. Wang, J., Huang, S., Huang, H., He, M., Wangyang, P., Gu, L. (2019). Effect of micro-groove on microstructure and performance of MAO ceramic coating fabricated on the surface of aluminum alloy. *Journal of Alloys and Compounds*, 777, 94–101. doi: <https://doi.org/10.1016/j.jallcom.2018.10.374>
44. Li, Z., Cai, Z., Cui, Y., Liu, J., Zhu, M. (2019). Effect of oxidation time on the impact wear of micro-arc oxidation coating on aluminum alloy. *Wear*, 426-427, 285–295. doi: <https://doi.org/10.1016/j.wear.2019.01.084>
45. Zhang, J., Kong, D. (2019). Effect of Micro-Arc Oxidation on Friction-Wear Behavior of Cold-Sprayed Al Coating in 3.5 wt. % NaCl Solution. *Journal of Materials Engineering and Performance*, 28 (5), 2716–2725. doi: <https://doi.org/10.1007/s11665-019-04076-1>